The Name of the Journal of the Journal
ISSN 2224-5774 (print) ISSN 2225-0492 (online)
Vol 2, No.4, 2012 

# Structural Design and Non-linear Modeling of a Highly Stable Multi-Rotor Hovercraft

Ali Shahbaz Haider[1*] Muhammad Sajjad[2]

1. Department of Electrical Engineering, COMSATS Institute of Information Technology, PO Box 47040, Wah Cantt, Pakistan
2. Department of Electrical Engineering, University of Engineering and Technology, Taxila, Pakistan

* E-mail of the corresponding author: engralishahbaz@gmail.com

**Abstract**

This paper presents a new design for a Multi-rotor Unmanned Air Vehicle (UAV). The design is based on the requirement of highly stable hover capability other than typical requirements of vertical takeoff and landing (VTOL), forward and sidewise motions etc. Initially a typical Tri-rotor hovercraft is selected for modeling and analysis. Then design modifications are done to improve the hover stability, with special emphasis on compensating air drag moments that exist at steady state hover. The modified structure is modeled and dynamic equations are derived for it. These equations are analyzed to verify that our structural modifications have the intended stability improvement effect during steady state hover.

**Keywords:** Multi-rotor Crafts, T-Copter, Rotational Matrix, Pseudo Inertial Matrix, Coriolis Acceleration, Air drag moment, Swash Plate

## 1. Introduction

The term UAV is used interchangeably with terms Auto Pilots or Self Piloted air craft's. UAVs are Unmanned Air Vehicles that can perform autonomous maneuvers hence are auto pilot based. They have got applications in military perspective as well as in civilian purposes. They are used for various functions such as surveillance, helicopter path inspection, disaster monitoring and land sliding observation, data and image acquisition of targets etc. (Salazar 2005, Jaimes 2008, Dong etc 2010 and Penghui 2010).This is the era of research and development of mini flying robot that may also act as a prototype for the controller design of bigger rotor crafts. Multi Rotor crafts have a lot of advantages over air planes and helicopter; they do not have swash plate and do not need any runway. Changing the speeds of motors with respect to each other, results in changing the flight direction of Multi rotors. They employ fixed pitch propellers, so are much cheaper and easy to control (Soumelidis 2008, Oosedo 2010 and Lee 2011). This research paper comprises of our work corresponding to tri rotor UAV Structure selection. There are various configurations possible as shown in figure 1. We have chosen the Tee structure, known as T-Copter. It has its own merit of somewhat decoupled dynamics in six degree of freedom as compared to other possible structures; moreover it is a challenging system to be modeled and controlled (Salazar 2005). we would show that replacing the tail rotor servo, which is used in most of the existing T-copter designs (Salazar 2005, Jaimes 2008, Dong 2010 and Penghui 2010), with air drag counter moment assembly has resulted in a much more simple model and precise control on the hover making the yaw control decoupled and independent.

## 2. T-Copter Dynamic Modeling

Structure of a typical tri-rotor hovercraft is shown in figure 2. It has two main rotors namely A and B and one tail rotor C. Roll $\phi$, pitch $\theta$ and yaw $\psi$ are defined in figure 3. In this typical configuration, tail rotor is at a tilt angle $\alpha$ which is adjustable by some sort of servo mechanism (Salazar 2005). This is usually done to have a component of force $F_3$ in $E_1E_2$-plane to compensate for net air drag moment in hovercraft body as explained in sections to follow. But this configuration has a severe drawback that it results in an acceleration of the body even in steady state. So first of all we would model structure of figure 2, then we

ISSN 2224-5774 (print) ISSN 2225-0492 (online)
Vol 2, No.4, 2012
will modify the structure so that we eliminate this effect, resulting in stable hover.

*2.1 Symbols and Terms*

Various symbols and terms used in the structure T-Copter in figure 2 and in its modeling equations, as described ahead, are enlisted below.

$\mathbb{R}$ =Real Space, $\varphi$ =roll, $\theta$ =Pitch, $\psi$ =yaw, M=mass of each rotor, $\omega$ =angular velocity

m=mass of entire Hovercraft Structure, $I \in \mathbb{R}^{3\times3}$ =Pseudo inertial matrix, $R \in \mathbb{R}^{3\times3}$ =Rotational matrix

$\beta(E_1, E_2, E_3)$ =Body Frame of Reference, $\Lambda(E_x, E_y, E_z)$ =Inertial Frame of Reference

C.G. =center of gravity of Hovercraft body

$\xi(x, y, z) \in \mathbb{R}^3$ =position of C.G in $\Lambda$

$\eta(\varphi, \theta, \psi) \in \mathbb{R}^3$ =Angular displacement vector of hovercraft body

$\ell_j$ =lengths of respective sides of hovercraft body

$F \in \mathbb{R}^3$ =force vector in $\beta$, $\tau \in \mathbb{R}^3$ =torque vector, $F_i$ =Force vector of the i$^{th}$ rotor

$\mathbb{Q} \in \mathbb{R}^3$ =parasitic moment term in system dynamics

$\mathbb{C} \in \mathbb{R}^3$ =parasitic acceleration term in system dynamics

*2.2 Newton-Euler's equations*

Newton-Euler's equations govern the dynamics of general multi rotor hovercrafts (Atul 1996, Francis 1998 and Barrientos 2009). These equations describe the dynamics of body in inertial frame of reference. These equations are as follows,

$$\begin{aligned} m\frac{d^2\xi}{dt^2}_{3\times1} &= R_{3\times3}F_{3\times1} - mg\ E_{z_{3\times1}} + \mathbb{C}_{3\times1}(\omega_b, \omega_i, r_j) \\ \mathrm{I}_{3\times3}\frac{d^2\eta}{dt^2}_{3\times1} &= \tau_{3\times1} + \mathbb{Q}_{3\times1}(\omega_b, \omega_i, r_j) \end{aligned} \qquad (1)$$

Where: $\xi = [x\ y\ z]^T$, $\eta = [\phi\ \theta\ \psi]^T$ and $E_z = [0 \quad 0 \quad 1]^T$

In the following sub sections we explain various terms within these equations, develop these equations for typical T-Copter. Then we would modify this structure so that resulting dynamic equations of modified structure are simple and well controllable.

2.2.1. Force Vector $F$

Forces on the structure in $\beta$ frame are shown in figure 4 in $E_2E_3$-plane. So the force vector comes out to be, $F = [0 \quad F_3 \sin\alpha \quad F_1 + F_2 + F_3 \cos\alpha]^T$

2.2.2 Rotational Matrix

Force vector F in Newton-Euler's equations is described with respect to body frame of reference $\beta$. In order to translate this vector in inertial frame of reference, a transformation matrix is needed, which is known as rotational matrix. Since body can perform three rotations with respect to inertial frame of reference, we have a possible of six rotational matrices $R_{\phi\theta\psi}, R_{\phi\psi\theta}, R_{\theta\phi\psi}, R_{\theta\psi\phi}, R_{\psi\phi\theta}, R_{\psi\theta\phi}$ .Out of the six of these possible transformation matrices; we select the standard one namely $R_{\psi\theta\phi}$ and denote it by R. This rotational matrix is given by,

$$R=\begin{bmatrix} \cos\theta\cos\psi & \sin\psi\cos\theta & -\sin\theta \\ \cos\psi\sin\theta\sin\phi-\sin\psi\cos\phi & \sin\psi\sin\theta\sin\phi+\cos\psi\cos\phi & \cos\theta\sin\phi \\ \cos\psi\sin\theta\sin\phi+\sin\psi\cos\phi & \sin\psi\sin\theta\sin\phi-\cos\psi\cos\phi & \cos\theta\cos\phi \end{bmatrix}$$

2.2.3 Parasitic forces vector $\mathbb{C}$

This vector includes the effects of centripetal and centrifugal acceleration of the structure and propellers. It also includes Coriolis acceleration terms.

2.2.4 Pseudo Inertial Matrix

Pseudo inertial matrix is a diagonal matrix of form,

$$\mathrm{I}=\begin{bmatrix} I_{roll} & 0 & 0 \\ 0 & I_{pitch} & 0 \\ 0 & 0 & I_{yaw} \end{bmatrix}$$

$I_{roll}$ Is moment of inertia of T-Copter for rotation around $E_1$ axis. $I_{pitch}$ is moment of inertia of T-Copter for rotation around $E_2$ axis. $I_{yaw}$ is moment of inertia of T-Copter for rotation around $E_3$ axis. Our structure is made up of cylindrical shells of radius "R". For a cylindrical shell of figure 5 with $\mathfrak{M}$ =mass of the shell, the principle moment of inertia are given by,

$$I_{xx}=\mathfrak{M}((3r^2+2h^2)/6)-\mathfrak{M}d^2,\quad I_{yy}=\mathfrak{M}((3r^2+2h^2)/6)-\mathfrak{M}d^2,\quad I_{zz}=3r^2$$

2.2.3.1. Moment of Inertia of T Structure

Now we derive the moment of inertia of the T structure of figure 6 during roll, pitch and yaw. The moment of inertia of the T structure during Roll i.e. rotation across E1 axis, as shown in figure 7.A, is denoted by $I_{E1,T}$. Using the results of multi body dynamics, it is sum of moment of inertia of shell 1 around E1 axis $I_{E1,S1}$ and shell 2 around E1 axis $I_{E1,S2}$.

$$I_{E1,T}=\{I_{E1,S1}\}+\{I_{E1,S2}\}$$

If $m_{s1}$ and $m_{s2}$ are masses of shell1 and shell2 then we get the following expression using parallel axis theorem,

$$I_{E1,T}=\{I_{E1,S1}\}+\{I_{E1,S2}\}=\{m_{S1}R^2\}+\{m_{S2}R^2/2+m_{S2}l_2^2/3\}$$

The moment of inertia of the T structure during pitch i.e. rotation across E2 axis, as shown in figure 7.B, is denoted by $I_{E2,T}$.

$$I_{E2,T}=\{I_{E2,S1}\}+\{I_{E2,S2}\}=\{m_{S1}R^2/2+m_{S1}(l_3^3+l_1^3)/(3(l_1+l_4))\}+\{m_{S2}R^2+[m_{S2}l_4^2]\}$$

The moment of inertia of the T structure during yaw i.e. rotation across E3 axis, as shown in figure 7.C, is denoted by $I_{E3,T}$.

$$I_{E3,T}=\{I_{E3,S1}\}+\{I_{E3,S2}\}=I_{E3,T}=\{m_{S1}R^2/2+m_{S1}(l_1^3+l_3^3)/(3(l_1+l_3))\}+\{m_{S2}R^2/2+m_{S2}l_2^2/3+[m_{S2}l_4^2]\}$$

2.2.3.2. Moment of Inertia of Motors

Motors are assumed to be solid cylinder of length $I_{mot}$, radius $R_{mot}$ and masses $m_{mot}$. During roll the situation is shown in figure 8.A. Moment of inertia of three motors during roll are given below,

$$I_{Mot1,roll}=m_{Mot}{R_{Mot}}^2/4+m_{Mot}l_{Mot}^2/3,\quad I_{Mot2,roll}=m_{Mot}{R_{Mot}}^2/4+m_{Mot}l_{Mot}^2/3+[m_{Mot}l_2^2]$$
$$I_{Mot3,roll}=m_{Mot}{R_{Mot}}^2/4+m_{Mot}l_{Mot}^2/3+[m_{Mot}l_{23}^2]$$

During pitch the situation is shown in figure 8.B. Moment of inertia of three motors during pitch are given below,

$$I_{Mot1,pitch} = m_{Mot}R_{Mot}{}^2/4 + m_{Mot}l_{Mot}^2/3 + [m_{Mot}l_3^2], \quad I_{Mot2,pitch} = m_{Mot}R_{Mot}{}^2/4 + m_{Mot}l_{Mot}^2/3 + [m_{Mot}l_4^2]$$
$$I_{Mot3,pitch} = m_{Mot}R_{Mot}{}^2/4 + m_{Mot}l_{Mot}^2/3 + [m_{Mot}l_4^2]$$

During yaw the situation is shown in figure 8.C. Moment of inertia of three motors during yaw are given below,

$$I_{Mot1,yaw} = m_{Mot}R_{Mot}{}^2/2 + [m_{Mot}l_3^2], I_{Mot2,yaw} = m_{Mot}R_{Mot}{}^2/2 + [m_{Mot}\ell_\gamma^2], I_{Mot2,yaw} = m_{Mot}R_{Mot}{}^2/2 + [m_{Mot}\ell_\gamma^2]$$

2.2.3.3. Moment of Inertia of the Control Unit Rack

Control unit rack holds the batteries, sensors and electronics boards etc. It is assumed to be in the form of a parallelepiped as shown in the figure 9. Its mass, including all parts placed in it, is $m_{rack}$. During roll, pitch and yaw, moment of inertia of rack are given to be.

$$I_{Rack,roll} = m_{Rack}(a^2 + 4c^2)/12, \quad I_{Rack,pitch} = m_{Rack}(b^2 + 4c^2)/12 + \left[m_{Rack}l_{rack}^2\right], \quad I_{Rack,yaw} = m_{Rack}(a^2 + b^2)/12 + \left[m_{Rack}l_{rack}^2\right]$$

2.2.3.4. Diagonal Elements of Pseudo Inertial Matrix

Results of multi body dynamics show that moment of inertia T-Copter during roll i.e. $I_{roll}$ is sum of moment of inertia of all parts of T-Copter during roll. Same is true for pitch and yaw moment of inertia, hence,

$$I_{roll} = I_{E1,T} + \sum_{i=1}^{3} I_{Moti,roll} + I_{Rack,roll}, \quad I_{pitch} = I_{E2,T} + \sum_{i=1}^{3} I_{Moti,pitch} + I_{Rack,pitch}$$
$$I_{yaw} = I_{E3,T} + \sum_{i=1}^{3} I_{Moti,yaw} + I_{Rack,yaw}$$

2.2.4. Nominal Torque Vector $\tau$

Figure 10 shows forces produced by propellers $P_1$, $P_2$ and $P_3$ on T-Copter body. Since torque is product of force and moment arm, so from figure 10, nominal torque vector comes out to be,

$$\tau = \left[\ell_2(F_2 - F_1) \quad -\ell_1(F_1 + F_2) + \ell_3 F_3 \cos\alpha \quad -\ell_3 F_3 \sin\alpha\right]^T$$

2.2.5. Parasitic Moment Vector $\mathbb{Q}$

Parasitic moments' vector contains all those moments that creep into the structure as a by-product of desirable moments. They are inevitable. Brief introduction of these moments is given in following sub sections. Expression for $\mathbb{Q}$ given by,

$$\mathbb{Q} = \mathrm{M}_g + \mathrm{M}_d + \mathrm{M}_f + \mathrm{M}_{ic}, \text{ where,}$$

$\mathrm{M}_g$ =Gyroscopic moment, $\mathrm{M}_d$ =Air Drag moment, $\mathrm{M}_f$ =Frictional moment, $\mathrm{M}_{ic}$ =Inertial Counter moment

2.2.5.1. Gyroscopic Moment

Consider figure 11 in which a rotating wheel is subjected to an angular acceleration $d\phi/dt$. It results in a gyroscopic moment orthogonal to both angular acceleration vector and angular velocity vector of rotating wheel. Expression for gyroscopic moment is given by,

$$\mathrm{M}_g = I\vec{\omega} \times \overrightarrow{(d\phi/dt)}$$

Gyroscopic moment is produced due to rotating propellers and rotors. If $I_{pc}$ is moment is inertia of rotor and propeller then gyroscopic moment vector, as denoted by $M_g$, is given by,

$$M_g = \begin{bmatrix} M_{gp} & M_{gr} & 0 \end{bmatrix}^T = I_{pc}\begin{bmatrix} (\omega_1+\omega_2-\omega_3)d\theta/dt & (\omega_1+\omega_2-\omega_3)d\phi/dt & 0 \end{bmatrix}^T$$

Here $M_{gr}$ is gyroscopic moment resulting from roll rate and $M_{gr}$ is gyroscopic moment resulting from pitch rate.

2.2.5.2. Air Drag Moment

These moments are produces as propellers rotate and drag through air. They are typically taken to be proportional to propellers' angular velocity squared, directed counter to direction of rotation of propellers. Denoting air drag moments by $Q$, we get the net air drag moment of the T-Copter, denoted by $M_d$, to be,

$$M_d = \begin{bmatrix} 0 & 0 & Q_1+Q_2-Q_3 \end{bmatrix}^T$$

2.2.5.3. Frictional Moments

Frictional moments are proportional to angular velocities. Frictional moment vector ( $M_f$ ), is given by,

$$M_f = k_f \begin{bmatrix} d\phi/dt & d\theta/dt & d\psi/dt \end{bmatrix}^T$$

Where $k_f$ =frictional constant

2.2.5.4. Inertial Counter moments

Inertial counter moment is proportional to rate of change of angular velocity of propellers. It acts only in yaw direction. Net inertial counter moment vector is given by,

$$M_{ic} = I_{pc}\begin{bmatrix} 0 & 0 & d\omega_1/dt + d\omega_2/dt - d\omega_3/dt \end{bmatrix}^T$$

Now the final expression for $\mathbb{Q}$ is given by,

$$\mathbb{Q} = \mathrm{M}_g + \mathrm{M}_d + \mathrm{M}_f + \mathrm{M}_{ic}$$

$$\mathbb{Q} = I_{pc}\begin{bmatrix} (\omega_1+\omega_2-\omega_3)\dot{\theta} \\ (\omega_1+\omega_2-\omega_3)\dot{\phi} \\ 0 \end{bmatrix} + \begin{bmatrix} 0 \\ 0 \\ Q_1+Q_2-Q_3 \end{bmatrix} + k_f \begin{bmatrix} \dot{\phi} \\ \dot{\theta} \\ \dot{\psi} \end{bmatrix} + I_{pc}\begin{bmatrix} 0 \\ 0 \\ \dot{\omega}_1+\dot{\omega}_2-\dot{\omega}_3 \end{bmatrix} \qquad (2)$$

*2.2.6. Developing Newton-Euler's Equations*

First of all we develop Newton's Equation,

$$m\frac{d^2\xi}{dt^2} = RF - mg\ E_z + \mathbb{C}$$

$$\Rightarrow m\frac{d^2}{dt^2}\begin{bmatrix} x \\ y \\ z \end{bmatrix} = R\begin{bmatrix} 0 \\ F_3\sin\alpha \\ F_1+F_2+F_3\cos\alpha \end{bmatrix} - mg\begin{bmatrix} 0 \\ 0 \\ 1 \end{bmatrix} + \begin{bmatrix} \mathbb{C}_x \\ \mathbb{C}_y \\ \mathbb{C}_z \end{bmatrix}$$

Letting $u_z = F_1+F_2+F_3\cos\alpha$ and putting value of R vector, we get the results as,

ISSN 2224-5774 (print) ISSN 2225-0492 (online)
Vol 2, No.4, 2012

$$m\frac{d^2x}{dt^2} = -u_z \sin\theta + (\sin\psi\cos\theta) F_3 \sin\alpha + \mathbb{C}_x$$
$$m\frac{d^2y}{dt^2} = u_z \cos\theta\sin\phi + (\sin\psi\sin\theta\sin\phi + \cos\psi\cos\phi) F_3 \sin\alpha + \mathbb{C}_y \quad (3)$$
$$m\frac{d^2z}{dt^2} = u_z \cos\theta\cos\phi - mg + (\sin\psi\sin\theta\sin\phi - \cos\psi\cos\phi) F_3 \sin\alpha + \mathbb{C}_z$$

Now we develop Euler's Equation,

$$I\frac{d^2\eta}{dt^2}I = \tau + \mathbb{Q} \Rightarrow \frac{d^2\eta}{dt^2} = I^{-1}\tau + I^{-1}\mathbb{Q} \Rightarrow \frac{d^2\eta}{dt^2} = I^{-1}\tau + I^{-1}\mathbb{Q} \Rightarrow \frac{d^2\eta}{dt^2} = I^{-1}\tau + I^{-1}\mathbb{Q}$$

Putting the values we get,

$$\frac{d^2}{dt^2}\begin{bmatrix}\phi\\ \theta\\ \psi\end{bmatrix} = \begin{bmatrix}I_\phi & 0 & 0\\ 0 & I_\theta & 0\\ 0 & 0 & I_\psi\end{bmatrix}^{-1}\begin{bmatrix}\ell_2(F_2 - F_1)\\ -\ell_1(F_1 + F_2) + \ell_3 F_3\cos\alpha\\ -\ell_3 F_3 \sin\alpha\end{bmatrix} + \begin{bmatrix}I_{roll}^{-1}\mathbb{Q}_\phi\\ I_{pitch}^{-1}\mathbb{Q}_\theta\\ I_{yaw}^{-1}\mathbb{Q}_\psi\end{bmatrix}$$

Or,

$$\frac{d^2\phi}{dt^2} = \frac{1}{I_\phi}\left[\ell_2(F_2 - F_1)\right] + I_{roll}^{-1}\mathbb{Q}_\phi$$
$$\frac{d^2\theta}{dt^2} = \frac{1}{I_\theta}\left[-\ell_1(F_1 + F_2) + \ell_3 F_3\cos\alpha\right] + I_{pitch}^{-1}\mathbb{Q}_\theta \quad (4)$$
$$\frac{d^2\psi}{dt^2} = \frac{1}{I_\psi}\left[-\ell_3 F_3 \sin\alpha\right] + I_{yaw}^{-1}\mathbb{Q}_\psi$$

Near to stability i.e. $\phi = 0$; $\theta = 0$; $d\phi/dt = 0$; $d\theta/dt = 0$; $d\psi/dt = 0$ and neglecting transient disturbance terms, Equation 2 becomes,

$$\mathbb{Q} = \begin{bmatrix}0 & 0 & Q_1 + Q_2 - Q_3\end{bmatrix}^T = \begin{bmatrix}0 & 0 & Q_{net}\end{bmatrix}^T$$

Equation set 3 becomes,

$$m\frac{d^2x}{dt^2} = \sin\psi F_3 \sin\alpha, \quad m\frac{d^2y}{dt^2} = \cos\psi F_3 \sin\alpha, \quad m\frac{d^2z}{dt^2} = u_z - mg - \cos\psi F_3 \sin\alpha \quad (5)$$

Equation set 4 becomes,

$$\frac{d^2\phi}{dt^2} = \frac{1}{I_\phi}\left[\ell_2(F_2 - F_1)\right], \quad \frac{d^2\theta}{dt^2} = \frac{1}{I_\theta}\left[-\ell_1(F_1 + F_2) + \ell_3 F_3\cos\alpha\right], \quad \frac{d^2\psi}{dt^2} = \frac{1}{I_\psi}\left[-\ell_3 F_3 \sin\alpha\right] + I_{yaw}^{-1}Q_{net}$$

(6)

Now it is evident from Equation set (5) and (6) that tail rotor tilt angle $\alpha$ ,that was introduced to compensate for $Q_{net}$ in equation set (6) has made accelerations in x, y and z directions dependent upon $\psi$ in a non-linear fashion and has made the model much complicated to control even near to the steady state

condition. Even at steady state, T-copter body would accelerate in xy-plane, a fact evident from equation set (5). Hence results in failure to achieve stable hover.

*2.2.7. Design Modification for Stable Hover*

Since $Q_{net}$ has comparatively very small magnitude, we can counter balance it by a small counter air drag couple by two small motors' set $M_{t,1}$ and $M_{t,2}$ as shown in the figure 12, and turn $\alpha$ =0. Two propellers of counter air drag couple motor assembly are chosen to be of opposite pitch so they rotate in opposite direction with equal speed. This would balance out their gyroscopic moments and air drag moments all the time. Moment of inertia for this counter air drag couple motor assembly can easily be calculated during roll, pitch and yaw by the procedure described above. Moment of inertia of this assembly can then be added in respective diagonal elements of Pseudo inertial matrix.

*2.2.8. Developing Newton-Euler's Equations for Modified T-Copter Structure*

If the distance between motors $M_{t,1}$ and $M_{t,2}$ is $\ell_t$ in figure 12 then moment produced by them has the magnitude $\ell_t F_t$, which is counter to air drag moment. So Equation set (3) becomes,

$$m\frac{d^2x}{dt^2} = -u_z \sin\theta + \mathbb{C}_x, \quad m\frac{d^2y}{dt^2} = u_z \cos\theta \sin\phi + \mathbb{C}_y, \quad m\frac{d^2z}{dt^2} = u_z \cos\theta\cos\phi - mg + \mathbb{C}_z \quad (7)$$

And equation set (4) becomes

$$\frac{d^2\phi}{dt^2} = \frac{1}{I_\phi}\left[\ell_2(F_2 - F_1)\right] + \mathbb{Q}_\phi, \quad \frac{d^2\theta}{dt^2} = \frac{1}{I_\theta}\left[-\ell_1(F_1 + F_2) + \ell_3 F_3\right] + \mathbb{Q}_\theta, \quad \frac{d^2\psi}{dt^2} = \frac{1}{I_\psi}\left[-\ell_t F_t\right] + \mathbb{Q}_\psi \quad (8)$$

An immense simplification in the structure dynamics is evident from equation sets (7) and (8) as compared to equation sets (3) and (4). Most of the nonlinearities of previous model are eliminated. Linear accelerations have been made decoupled from yaw angle as clear from equation set (7).Now we observe the behaviour near to steady state i.e. $\phi = 0;\ \theta = 0;\ d\phi/dt = 0;\ d\theta/dt = 0;\ d\psi/dt = 0$

Neglecting transient disturbance terms, equation set (7) becomes,

$$m\frac{d^2x}{dt^2} = 0, \quad m\frac{d^2y}{dt^2} = 0, \quad m\frac{d^2z}{dt^2} = u_z - mg \quad (9)$$

Equation set (8) becomes,

$$\frac{d^2\phi}{dt^2} = \frac{1}{I_\phi}\left[\ell_2(F_2 - F_1)\right], \quad \frac{d^2\theta}{dt^2} = \frac{1}{I_\theta}\left[-\ell_1(F_1 + F_2) + \ell_3 F_3\right], \quad \frac{d^2\psi}{dt^2} = \frac{1}{I_\psi}\left[-\ell_t F_t\right] + Q_{net} \quad (10)$$

So we see that our structural modification has resulted in an extremely stable model near to steady state which is evident from equation sets (9), (10) as compared to equation set (5) and (6).

## 5. Conclusion

In typical Tri-rotor Hovercrafts, air drag moments of propellers are compensated by tilting the tail rotor through an angle, by using some sort of servo mechanism. Such arrangement results in an unstable steady state hover and much more complicated system dynamics. If tail rotor servo mechanism is replace by a cheap counter air drag couple motors' assembly, we get immensely simple system dynamics and completely stable steady state hover.

**References**

Atul Kelkar & Suresh Joshi (1996) *Control of Nonlinear Multibody Flexible Space Structures*, Lecture Notes in Control and Information Sciences, Springer-Verlag London Publications.

Barrientos, A.; Colorado, J. (22-26 June 2009). Miniature quad-rotor dynamics modeling & guidance for vision-based target tracking control tasks. *Advanced Robotics, 2009. ICAR 2009. International Conference on* , vol., no., pp.1-6

Dong-Wan Yoo; Hyon-Dong Oh; Dae-Yeon Won; Min-Jea Tahk. (8-10 June 2010). Dynamic modeling and control system design for Tri-Rotor UAV. *Systems and Control in Aeronautics and Astronautics (ISSCAA), 2010 3rd International Symposium on* , vol., no., pp.762-767

Francis C.Moon (1998) *Applied Dynamics With Application to Multibody Systems*, Network Books, A Wiley-Interscience publications.

Jaimes, A.; Kota, S.; Gomez, J. (2-4 June 2008). An approach to surveillance an area using swarm of fixed wing and quad-rotor unmanned aerial vehicles UAV(s). *System of Systems Engineering, 2008. SoSE '08. IEEE International Conference on* , vol., no., pp.1-6

Lee, Keun Uk; Yun, Young Hun; Chang, Wook; Park, Jin Bae; Choi, Yoon Ho. (26-29 Oct. 2011). Modeling and altitude control of quad-rotor UAV. *Control, Automation and Systems (ICCAS), 2011 11th International Conference on* , vol., no., pp.1897-1902

Oosedo, A.; Konno, A.; Matumoto, T.; Go, K.; Masuko, K.; Abiko, S.; Uchiyama, M. (21-22 Dec. 2010). Design and simulation of a quad rotor tail-sitter unmanned aerial vehicle. *System Integration (SII), 2010 IEEE/SICE International Symposium on* , vol., no., pp.254-259

Penghui Fan; Xinhua Wang; Kai-Yuan Cai. (9-11 June 2010). Design and control of a tri-rotor aircraft. *Control and Automation (ICCA), 2010 8th IEEE International Conference on* , vol., no., pp.1972-1977

Salazar-Cruz, S.; Lozano, R. (18-22 April 2005). Stabilization and nonlinear control for a novel Tri-rotor mini-aircraft," *Robotics and Automation, 2005. ICRA 2005. Proceedings of the 2005 IEEE International Conference on* , vol., no., pp. 2612- 2617

Soumelidis, A.; Gaspar, P.; Regula, G.; Lantos, B. (25-27 June 2008). Control of an experimental mini quad-rotor UAV. *Control and Automation, 2008 16th Mediterranean Conference on* , vol., no., pp.1252-1257

 

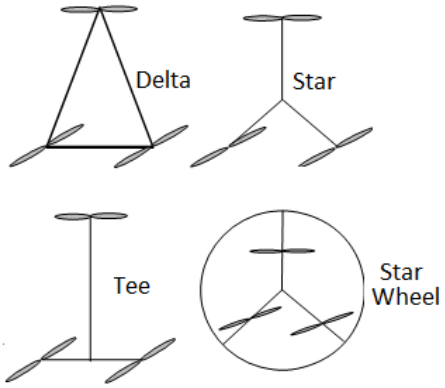


Figure 1. Possible Tri-rotor Craft Structures (structures' topological names are indicated)

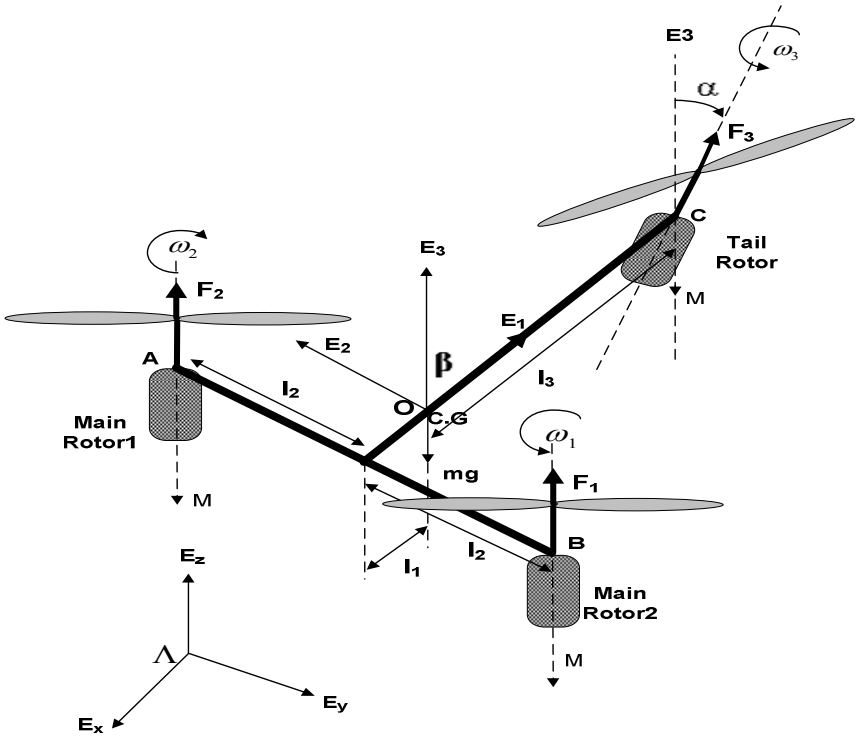


Figure 2. T-Copter Structure and Parameters

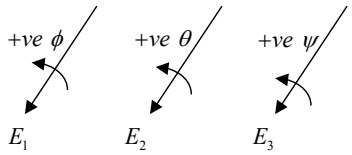


Figure 3. Roll, Pitch and yaw definitions

 

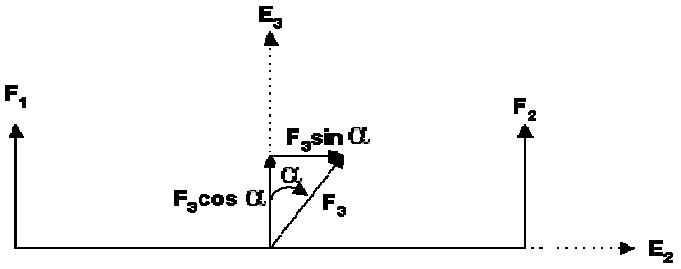


Figure 4. Forces on structure in body frame

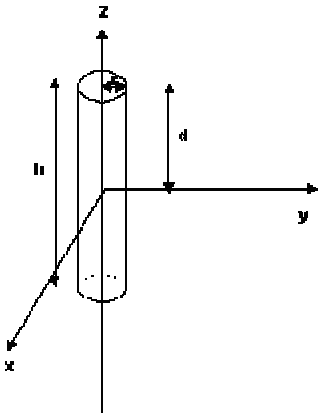


Figure 5. A cylindrical shell

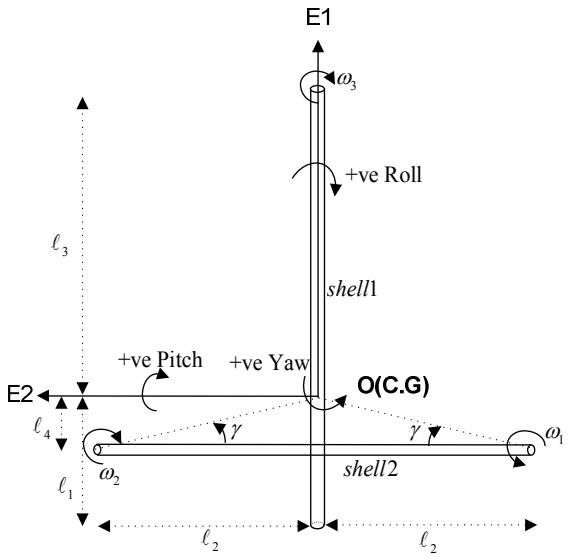


Figure 6. T structure made up of cylindrical Shells

 

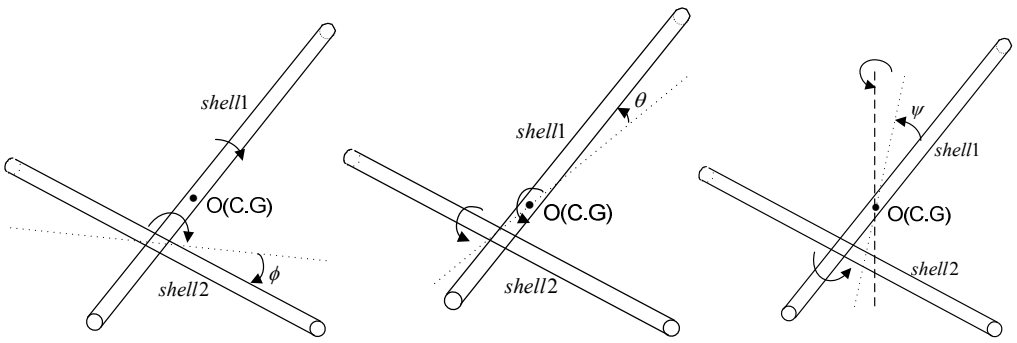


A. T structure during roll B. T structure during pitch C.T structure during yaw

Figure 7. T structure during three angular rotations in space

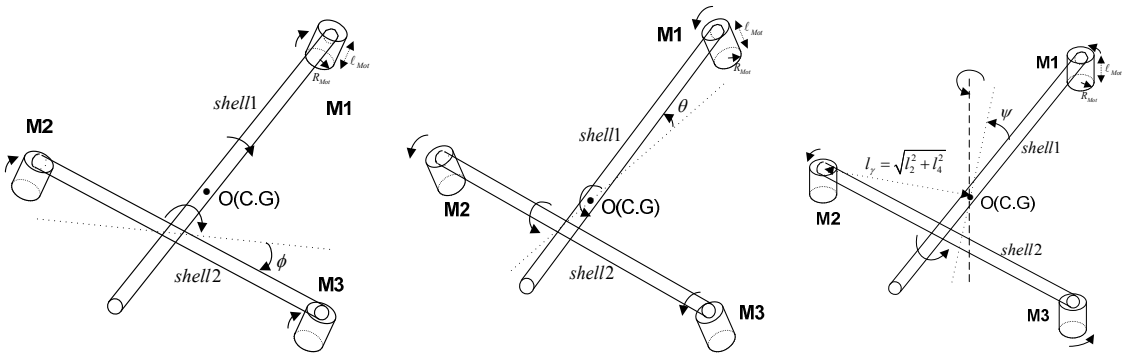


A. Motors during roll B. Motors during pitch C. Motors during yaw

Figure 8. Motors during three angular rotations in space

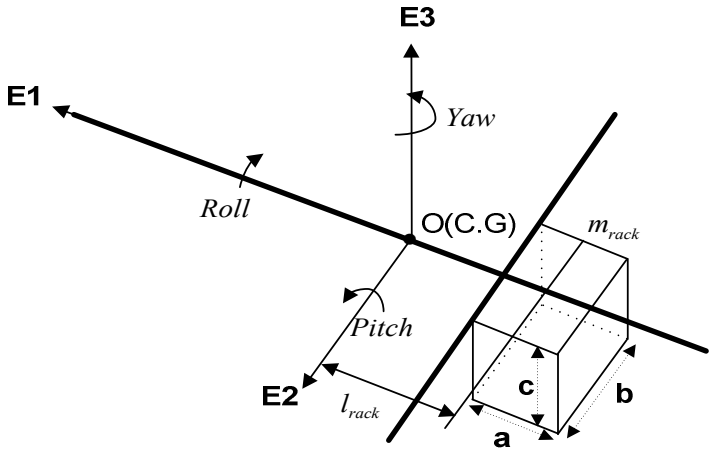


Figure 9. Control unit rack

 

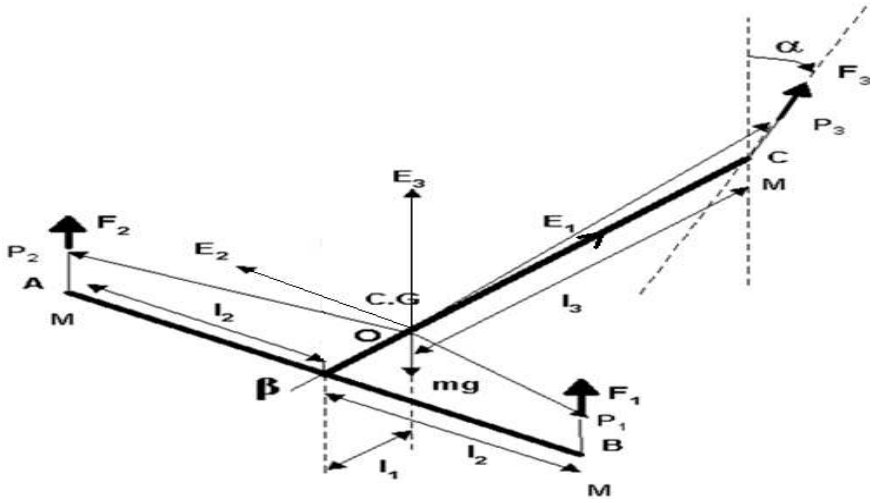


Figure 10. Force Diagram for Torque vector on T-Copter.

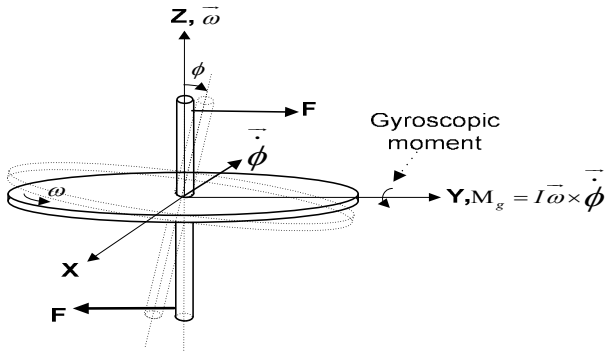


Figure 11. Gyroscopic moments

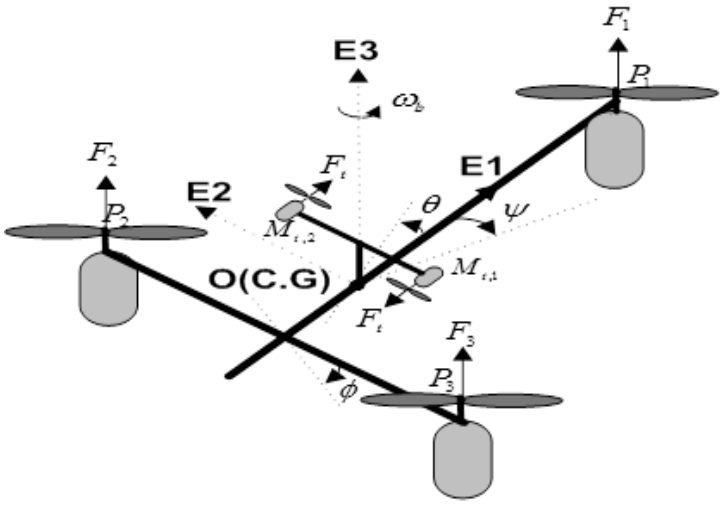


Figure 12. Modified T-copter Structure